Advances in Geo-Energy Research

Vol. 13, No. 2, p. 132-145, 2024

Original article

Tensile behavior and damage mechanisms of hot dry rock under thermal shock fatigue and seawater dissolution

Cunbao Li[1,2], Jiahui Tu[1,2], Heping Xie[1,2], Jianjun Hu[1,3]*

[1]*State Key Laboratory of Intelligent Construction and Healthy Operation and Maintenance of Deep Underground Engineering, Shenzhen University, Shenzhen 518060, P. R. China*

[2]*Guangdong Provincial Key Laboratory of Deep Earth Sciences and Geothermal Energy Exploitation and Utilization, Institute of Deep Earth Sciences and Green Energy, College of Civil and Transportation Engineering, Shenzhen University, Shenzhen 518060, P. R. China*

[3]*Key Laboratory of Deep Earth Science and Engineering (Sichuan University), Ministry of Education, Chengdu 610065, P. R. China*

Keywords:
Hot dry rock
brazilian splitting
heat treatment
seawater thermal shock
acoustic emission tests

Cited as:
Li, C., Tu, J., Xie, H., Hu, J. Tensile behavior and damage mechanisms of hot dry rock under thermal shock fatigue and seawater dissolution. Advances in Geo-Energy Research, 2024, 13(2): 132-145.
https://doi.org/10.46690/ager.2024.08.07

Abstract:
Significant potential exists for mining hot dry rock in coastal areas, oceans, islands, and reefs by utilizing abundant seawater as a heat-exchanging medium. It is crucial for optimizing reservoir stimulation technology to explore mechanical characteristics and mechanisms for damage of reservoir rocks during seawater mining of hot dry rock. In this research,granite was subjected to several heat treatment temperatures (100 to 500 °C) and various numbers of fatigue thermal shocks (0-20) using seawater before Brazilian splitting tests and acoustic emission testing. The findings show that temperature, the thermal shocks, and seawater dissolution are the main factors influencing granite's tensile strength.The temperature threshold for significant degradation of tensile strength, resulting from thermal shock from seawater and heat treatment, ranges from 200 to 300 °C. At high temperatures (300 to 500 °C), seawater decreases the tensile strength of granite by approximately 1.67 times compared to freshwater in cycles 0-10, and by about 3.20 times in cycles 10-20. In general, the higher the temperature and frequency of seawater impact, the greater the plasticity of the rock, the lower the tensile strength, and the higher the cumulative count and energy of acoustic emission. The number of seawater thermal shocks and granite's tensile strength have a negative link that is substantially amplified by the temperature. The double effects of seawater cold cycle and heat treatment temperature cause granite to become more porous and progressively shift from tensile to shear damage. These results provide a benchmark for utilizing seawater as a thermogenic medium in enhanced geothermal systems for mineral extraction procedures.

1. Introduction

The necessity of discovering and employing new green energy sources has increased due to the depletion of non-renewable resources (Kumari et al., 2018a). Owing to their cleanliness, abundant reserves, and wide distribution globally, geothermal resources exhibit potential for development (Zhang et al., 2019; Pathiranagei et al., 2021; Hu et al., 2022). Hot dry rock (HDR) has also drawn much interest as a major geothermal resource (Pan et al., 2019; Li et al., 2020). Generally, HDR is stored underground at 3-10 kilometer depths (Huang, 2012). With increasing depth, HDR exhibits elevated temperatures, impeding the extraction of the heat resource. Ideal conditions for mining HDR are profundities of 5-6 km underneath the surface and temperatures extending from 150 to 500 °C (Breede et al., 2013). These specified criteria position granite as one of the main geological formations suitable for HDR development.

The extraction of HDR geothermal energy is commonly accomplished through the use of enhanced geothermal systems (EGS) (Bertani, 2016; Asai et al., 2019). The physical characteristics of HDR (like its density, wave speed, modulus of elasticity, and tensile strength) are impacted by the heat exchange

Yandy Scientific Press

*Corresponding author.
E-mail address: cunbao.li@szu.edu.cn (C. Li); 2200471037@email.szu.edu.cn (J. Tu); xiehp@szu.edu.cn (H. Xie); hujianjun@cumt.edu.cn (J. Hu).

Received June 16, 2024; revised July 7, 2024; accepted July 26, 2024; available online July 30, 2024.

process between the high-temperature rock reservoir and the low-temperature heat extraction medium in the development of HDR geothermal energy (Rong et al., 2018; Hu et al., 2021; Zhu et al., 2021). The physical and mechanical qualities of HDR are highly variable because of variations in the high-temperature rock reservoir's mineral composition, temperature range, extraction heat medium, and cooling technique (Chen et al., 2017; Zhang et al., 2021; Li et al., 2022; Ma et al., 2022; Xi et al., 2023). Multiple cycles of water cooling within an EGS can considerably alter the HDR storage bedrock's pore structure and internal composition of minerals (Salimzadeh et al., 2018; Shi et al., 2020; Yin et al., 2020, 2022; Zhao et al., 2020). Understanding the mechanical performance and degradation mechanisms of HDR following cyclic water cooling is necessary for the stable development and utilization of geothermal resources.

In conventional EGS geothermal energy extraction, substantial freshwater resources are necessary for heat extraction (Gérard et al., 2006). Thus, in regions where freshwater resources are limited, including coastal areas and islands, freshwater conservation should be taken into account when extracting geothermal energy. The Greater Bay Area of Guangdong, Hong Kong, Macao possesses abundant marine and geothermal resources (Zolfaghari et al., 2023), offering great potential for development through the use of seawater to be a medium for heat extraction. It is still unknown how HDR's tensile behaviour evolved when it used saltwater as a heat extraction medium. Therefore, it is necessary to investigate the mechanical behavior of HDR during seawater heat extraction as well as the usage of seawater as the heat exchange medium.

Numerous studies have examined the mechanical behavior of granites under varying temperatures. Acoustic emission (AE) analysis, a method for material damage detection and evaluation (Watanabe et al., 2001; Venturini and Dulieu-Barton, 2006; Sagar et al., 2012; Ding et al., 2016; Ran et al., 2024), can accurately determine rock damage behavior (Filipussi et al., 2015). This approach is commonly used for rock damage detection (Ge and Sun, 2018; Sha et al., 2020; Yin et al., 2021). Additionally, AE can be used to assess how temperature affects granite damage and cracking processes, including the change from brittle to ductile processes (Gautam et al., 2018). Yang et al. (2017) examined how high temperatures affected granite's compressive strength and found that it decreased as temperature rose. They provided a microscopic explanation of the granite damage mechanism. Kumari et al. (2017, 2018b) determined the impact of different cooling speeds on granite's mechanical behavior and the corresponding crack expansion patterns by treating high-temperature Australian Strathbogie granite and analyzing AE results. The outcome demonstrated that quenching induces crack development in the rock, leading to thermal damage. Siratovich et al. (2015) tested high-temperature rocks with water quenching, and they discovered that the permeability of the rocks increased significantly as the thermal stress increased. Granite saw substantial changes in its mechanical and physical properties during high-temperature water-cooling cycles. (Weng et al., 2020; Zhu et al., 2020a, 2020b). The relationship between wave velocity, granite's elastic modulus, and uniaxial compressive strength was investigated by Zhu et al. (2021) across varying numbers of heating-water cooling cycles. Rong et al. (2018) and Yu et al. (2020) studied how the mechanical and physical characteristics of granite and marble were affected by cycles of heating and cooling water. Uniaxial compression tests were performed for analysis utilizing AE detection methods and microscopic methods. The impact of temperature and the quantity of water-cooling cycles on granite damage was evaluated by Zhu et al. (2018, 2022). They discovered correlations between critical AE parameters. They established a rock damage equation and a thermal impact stress equation based on AE detection results. Finally, Van Berk et al. (2015) predicted the regions where reservoir porosity and permeability fluctuate using three-dimensional modeling approaches, owing to seawater injection-induced dissolution or precipitation of minerals. Deng et al. (2023) identified regions of thermal damage in granite at varying temperatures and seawater thermal impact durations using fractal dimension analysis. Hu et al. (2024) used fractal theory analysis and nuclear magnetic resonance methods to conclude that the combined effects of thermal fatigue and seawater can significantly increase reservoir permeability. Their study demonstrates that there is a lot of promise to use seawater as a medium of heat extraction for HDR. But the process by which HDR's mechanical characteristics evolved during seawater fatigue and thermal shock remains unknown.

In summary, exploring the tensile behavior of HDR under seawater fatigue thermal shock is extremely important practically for the development of HDR using seawater as the heat extraction medium. Therefore, in this study, granite treated with different heating temperature treatments and number of fatigue thermal shocks were subjected to seawater Brazilian splitting tests. Their effects on the granite's tensile behavior during the tests were examined. AE analysis was used to monitor test specimens during cleavage. The differential characteristics of the cleavage damage process in granite after it was subjected to varying temperatures and different numbers of thermal impacts from seawater were evaluated by analyzing changes in AE parameters like count and energy. In addition, damage parameters D and RA (rise time/amplitude)/AF (average frequency) were characterized using AE data for describing the process of degradation and the type of damage to the rock. The study findings can potentially serve as a valuable benchmark for using seawater as a heat extraction medium in EGS mining.

2. Methods

2.1 Sample preparation

The firm, grayish brown test granite used in the tests had an initial density of 2.617 g/cm^3. Fig. 1(a) displays the main components of the granite as determined by X-ray diffraction investigation. Samples were extracted from the same whole rock mass to maintain consistency in the sample extraction process, which helped to ensure experiment accuracy and minimize variation across granite samples, and all samples had no visible cracks. Following ISRM specifications for the Brazil splitting test, 52 standard cylinder samples measuring

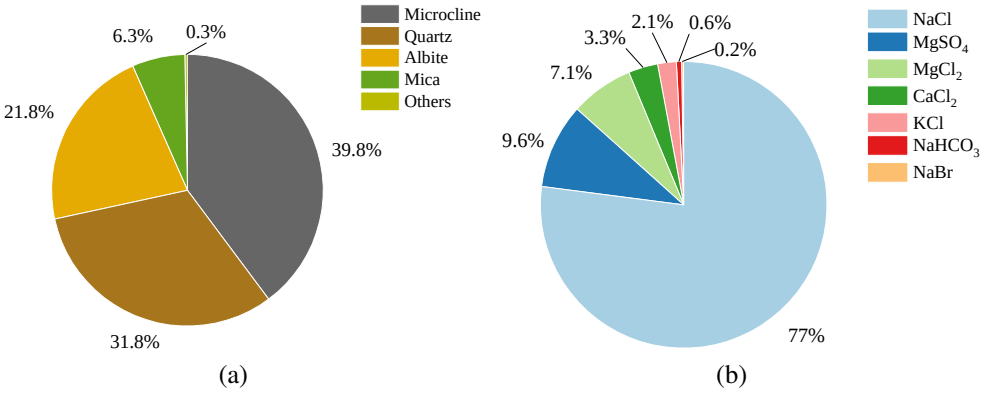

Fig. 1. Main elements of (a) the test granite and (b) the simulated seawater.

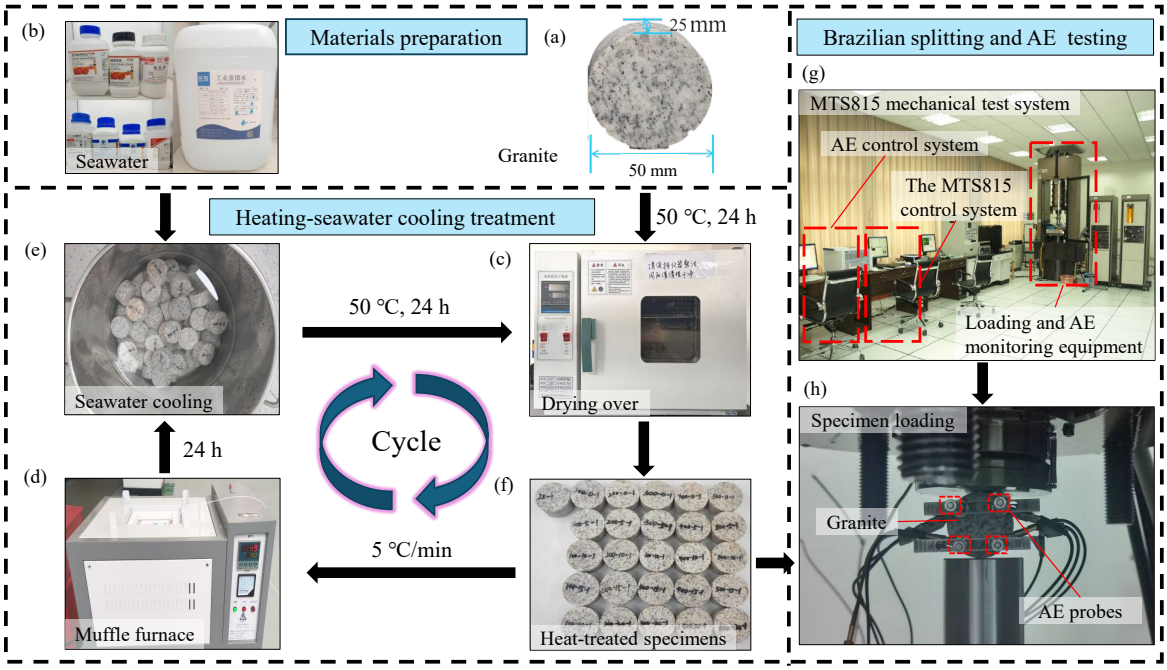

Fig. 2. Schematic of the experimental process in this study.

25 mm in height and 50 mm in diameter were prepared.

In the experiment, simulated seawater was prepared following the standard established by the Third Institute of Oceanography of the State Oceanic Administration of China, reflecting the properties of southeast coastal seawater. The resulting ion concentration in the seawater is illustrated in Fig. 1(b).

2.2 Experimental process and equipment

In order to guarantee the precision of the experimental results and reduce the influence of sample error, we divided 50 samples into 25 groups, each comprising 2 samples in each group. Subsequently, 2 samples were tested for Brazilian cleavage without treatment, serving as a control group. Mean values of the test results were then used to represent each sample group. Fig. 2 showed the experimental process. Wthin each group, these specimens were heated to predefined temperatures (100, 200, 300, 400 and 500 °C) and subjected to a specified number of fatigue thermal shocks (0, 5, 10, 15 and 20) before the Brazilian split test was applied and AE characteristic signals collected.

The experimental steps were as follows:

1) A specimen was placed in a 101-00B electric thermostatic drying oven set to 50 °C for 24 h (Fig. 2(c)).
2) The prepared standard specimen was placed in CR-MJ5 muffle furnace with the following settings: Maximum temperature range, 500 °C; voltage, 220 V; power, 2 kW (Fig. 2(d)), and then heated at a rate of 5 °C/minute until the test temperature was attained.
3) To guarantee that the sample temperature was consistent, the furnace temperature was maintained for 4 hours.
4) Using tongs, the hot sample was taken out of the furnace and quickly cooled by submerging it in room-temperature seawater (Fig. 2(e)). After 24 h, and the sample had

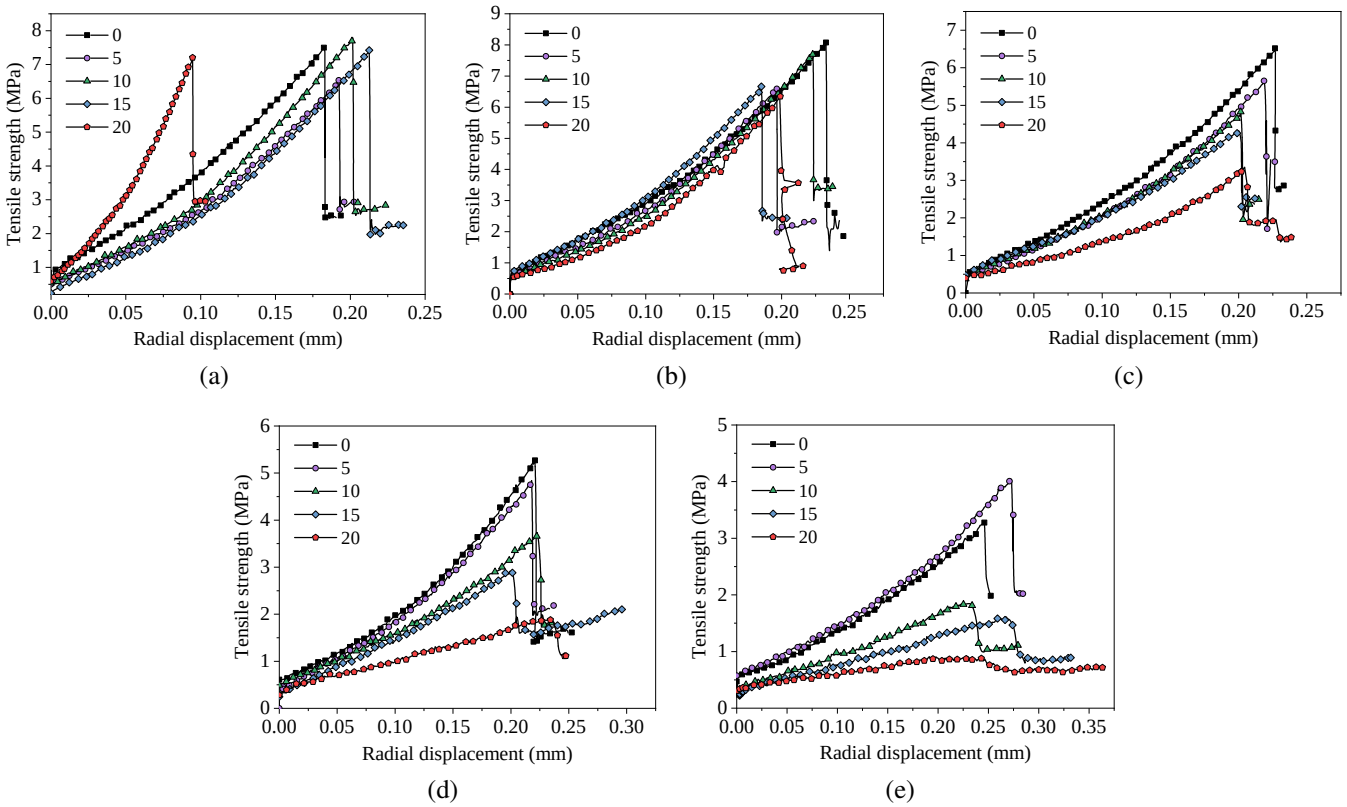

Fig. 3. Stress-displacement (radial displacement) curves of granite subjected to various treatment temperatures and different thermal shock cycle counts by using seawater. (a) 100 °C, (b) 200 °C, (c) 300 °C, (d) 400 °C and (e) 500 °C.

cooled to ambient temperature (25 °C), it was removed from the seawater and dried for a further 24 h at 50 °C in the drying oven.

5) This procedure completed 1 thermal shock cycle, and Steps 1-4 were repeated to achieve the required number of shock cycles. In addition, the specimens that had to be subjected to 0 cycles only needed to be cooled naturally for 24 h, as described in Step 3, without being placed in the drying oven to remove moisture.

After being exposed to the required number of seawater thermal shocks at each predetermined temperature, each granite sample underwent a Brazilian splitting test using an MTS815 rock mechanics test system (Fig. 2(g)) at the Key Laboratory of Sichuan University. The system's maximum compression displacement was 100 mm, its maximum axial load was 4,600 kN. AE characteristic parameters and waveform analyses were then collected using the PCI-II AE system. The loading mode of the MTS815 rock mechanics test system was set to "displacement", and the loading rate of it was 0.025 mm/min. Eight Micro30S AE sensors, with an AE threshold of 35 dB, were placed on each sample (Fig. 2(h)). To ensure optimal probe-sample contact between the probes and a sample, we coated the AE probes with an appropriate amount of petroleum jelly (Vaseline) to enhance signal acquisition and reduce test errors.

3. Results and analysis

3.1 Stress-displacement curves

Fig. 3 presented granite's stress-displacement curves at varying numbers of fatigue thermal shocks and heat treatment temperatures. Comparing all the plots reveals that the differences in the stress-displacement curves under various seawater fatigue thermal shocks become increasingly apparent as the granite's heat treatment temperature rises-that is, the rise in temperature heightens the effect of seawater thermal shock on these specimens. For instance, at temperatures of 100 or 200 °C and the frequency of seawater cycles between 0 and 20, the change of the stress-displacement curves for the specimen were not obvious and no apparent regularity. However, in particular, the slope of the curve increases significantly at a temperature of 100 °C for 20 cycles, while the tensile strength remains essentially unchanged. When the test temperature surpassed 300 °C, the stress-strain curves started to exhibit noticeable variations as the number of thermal shocks from seawater increased. The slope and the maximum displacement of the curves gradually decreased and began to rise respectively. In addition, the stress-displacement curves changed from concave to convex, the brittleness of the granite decreased, the plasticity was enhanced, and the granite was transformed from plastic-elastic to plastic-elastoplastic. These observations suggest that under the aforementioned conditions, heat treatment temperature between 200 to 300

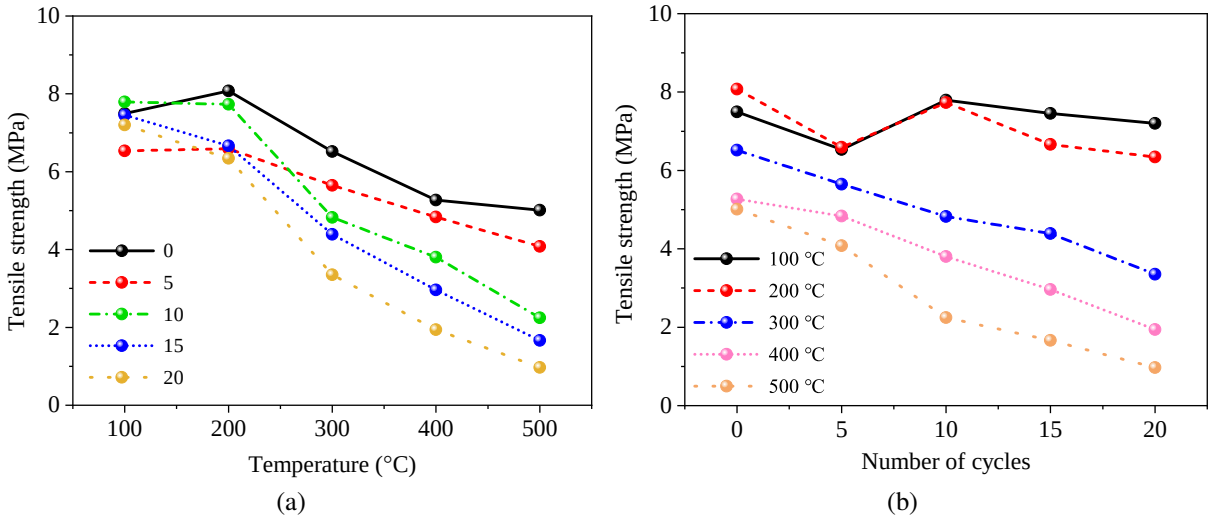

Fig. 4. Tensile strength curves under various (a) treatment temperatures and (b) numbers of seawater thermal shocks (cycles).

°C, the existence of seawater thermal shock effect on granite damage to a limit temperature, more than the temperature, seawater thermal shock on damage to granite increased in severity.

3.2 Tensile strength

The stretching properties of the test specimens were evaluated using tensile strength curves (Fig. 4). The influence of temperature on the tensile strength of samples subjected to different cycles is shown in Fig. 4(a). When the temperature rises, the tensile strength of samples in 0 and 5 cycles first increases and then decreases. Conversely, as the temperature increases, specimens subjected to 10 to 20 cycles exhibit a consistent, linear decrease in tensile strength. Notably, specimens under low cycle circumstances (0-10) exhibit a notable loss in tensile strength at 300 °C. In addition, regarding temperatures between 100 and 200 °C, the tensile strength completes the transition from an increasing to a decreasing trend from 0 to 10 cycles. For specimens without cycling (cycle 0), when the heat treatment temperature was low, newborn cracks had not yet been produced in the granite, and the minerals within the granite expanded, filling some pores (Zuo et al., 2011). This expansion increases contact area and pressure on mineral surfaces, thereby enhancing friction and improving tensile strength. In specimens subjected to 5 low cycles, thermal stresses result in microcracking, which inhibits the rapid propagation of main cracks and enhances overall crack resistance (Shao et al., 2022; Chen et al., 2023). However, for specimens exposed to 10 or more high cycles, increased temperature results in the generation of greater and more frequent thermal stresses, which facilitate microcrack interconnection, increasing the likelihood of specimen damage and consequently reducing tensile strength. In addition, the decreasing slope of the tensile strength curve from 200 to 500 °C becomes steeper with an increasing number of cycles at low cycles (0-10). This is due to greater microcrack connectivity resulting from higher thermal stresses at higher cycles. What is more, the tensile strength across different cycles decreases significantly with the temperature threshold is reached during the temperature increases between 200 and 300 °C. During this period, thermal stress increases substantially, causing the specimen's micro cracks to link with one another, ultimately compromising the integrity of the granite.

The granite exposed to high treatment temperatures exhibited reduced overall tensile strength and the degradation effect of seawater was more evident as the quantity of cycles rises (Fig. 4(b)). This corresponds to the temperature threshold at which seawater thermal shock to the specimen begins to have a noticeable effect. The tensile strength curves showed fluctuations with an increase in the frequency of cycles when the granite's heat treatment temperature was adjusted between 100 and 200 °C. This fluctuation suggests the potential for enhancing the samples' tensile strength through cycles induced by seawater. When the number of cycles increased from 0 to 5 times, the tensile strength of the samples subjected to different temperatures dropped (Fig. 4(b)). This reduction demonstrates that the initial thermal impact of seawater exerted a serious damaging effect on the granite. However, the specimens' tensile strength dramatically reduced as the number of cycles rised when the heating temperature was raised to 300 °C or higher, and this downward trend was nearly linear. As the treatment temperature rises, the minerals' non-homogeneous thermal expansion and thermal shock effects encourage the development of cracks, increasing the granite's porosity and permeability (Hu et al., 2021). This further highlights the pronounced detrimental impact of seawater on granite at high temperatures. Notably, between 5 and 10 cycles, granite's tensile strength rises at lower temperatures (100 and 200 °C), but decreases at higher temperatures (300 to 500 °C). The primary reason for this behavior is the pronounced role of thermal shock and crack evolution in granite at elevated temperatures. At higher temperatures, pre-existing cracks in the specimen exert less influence; thus, the more cycles applied, the greater the damage, resulting in reduced tensile

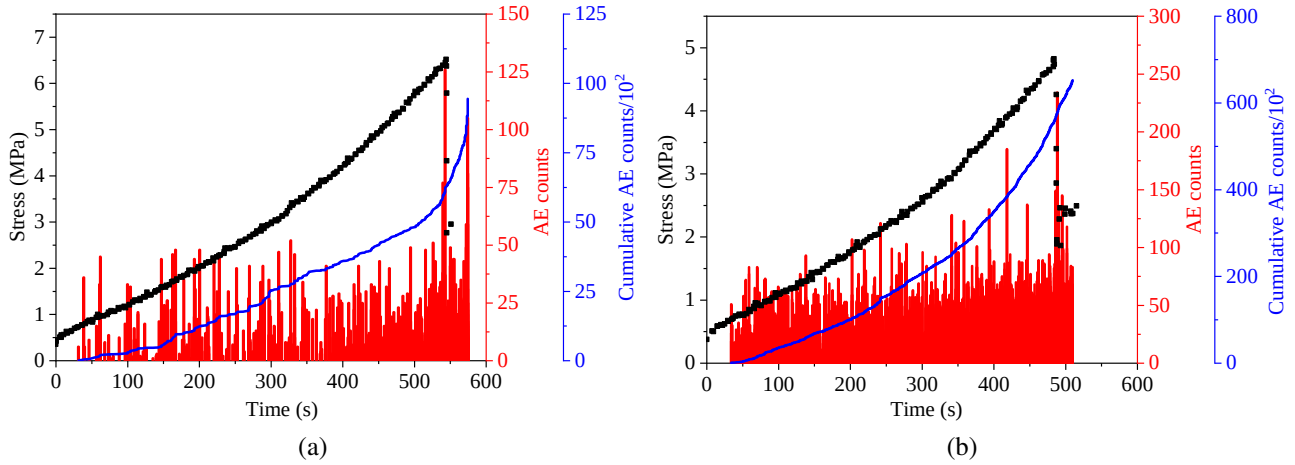

Fig. 5. Curves of stress, AE count, and cumulative AE count over time for various numbers of seawater thermal shock cycles at a treatment temperature of 300 °C. (a) 0 and (b) 10 cycles.

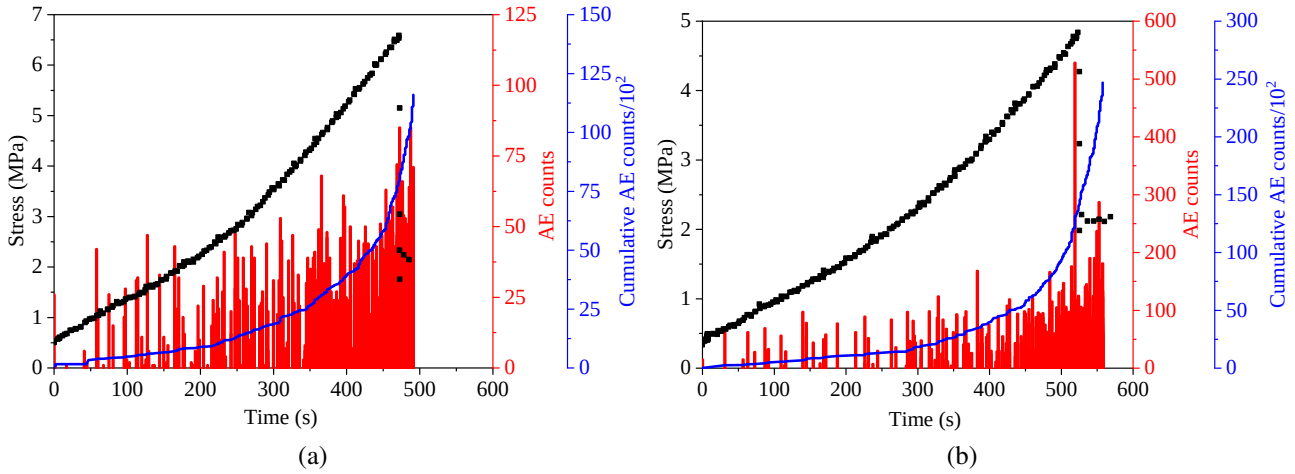

Fig. 6. Curves of stress, AE count, and cumulative AE count over time for various treatment temperatures and 5 seawater thermal shock cycles. (a) 200 °C and (b) 400 °C.

strength. Conversely, at lower temperatures, the impact of thermal damage is less significant. Here, initial crack closure and the formation of new cracks occur, leading to a relatively smaller change in tensile strength compared to the changes in the discrete nature of rock cracks. This phenomenon makes it possible for cyclic loading to increase the tensile strength at low temperatures. Additionally, the chemistry of seawater may enhance the tensile strength in the circumstances of lower thermal shock.

In summary, three main reasons are responsible for the notable decline in granite's tensile strength: Heating temperature, the quantity of cycles, and seawater dissolution.

3.3 Tensile load, AE count, and cumulative AE count

In this study, the granite damage mechanism was explored using AE parameters. Thus, the typical AE count and the stress change characteristics of the test samples were analyzed after different numbers of seawater fatigue thermal shocks (0 and 10) and treatment temperature (200 and 400 °C) (Figs. 5 and 6).

The time curves of AE parameters and stress for specimens indicated a high correlation during loading (Figs. 5 and 6). As the temperature of heat treatment rises and the quantity of thermal shocks caused by seawater fatigue increases, the AE count exhibited an upward trend over loading time until the specimen reached its ultimate tensile strength. The AE count was primarily concentrated near the ultimate load, with the maximum AE count occurring when the specimen was approaching failure. This finding implies that the AE response was weak at the beginning of the compression phase but became intensified close to the ultimate tensile stress. This observation coincided with the production of more and larger cracks in the structure, resulting in more serious damage to the specimen. As the specimen loading time increased, the AE cumulative count gradually increased, indicating that the specimen was slowly accumulating internal damage before the failure. In addition, internal cracks gradually developed until

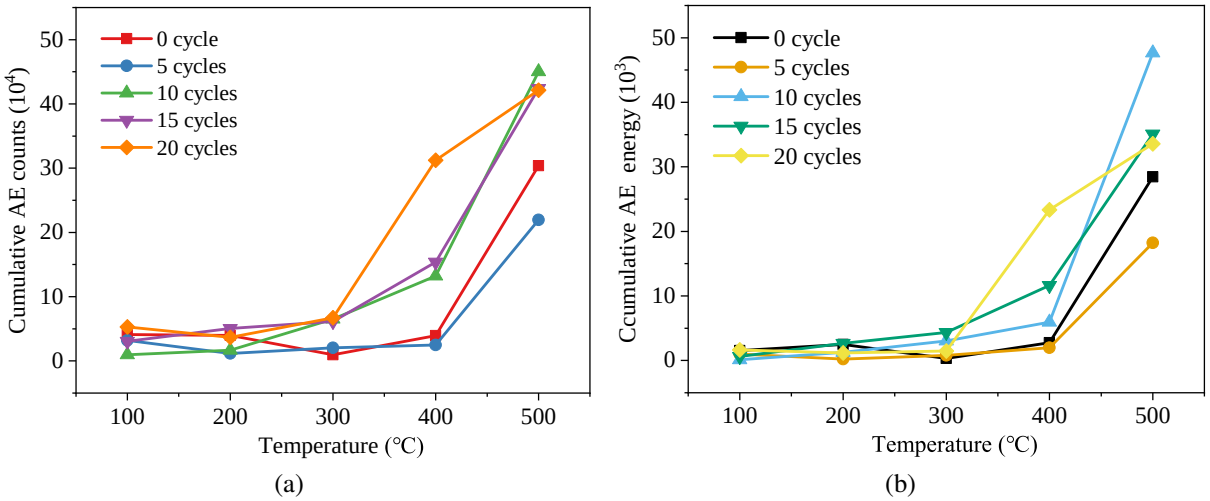

Fig. 7. Relationships between (a) cumulative AE count and (b) cumulative AE energy with respect to treatment temperature.

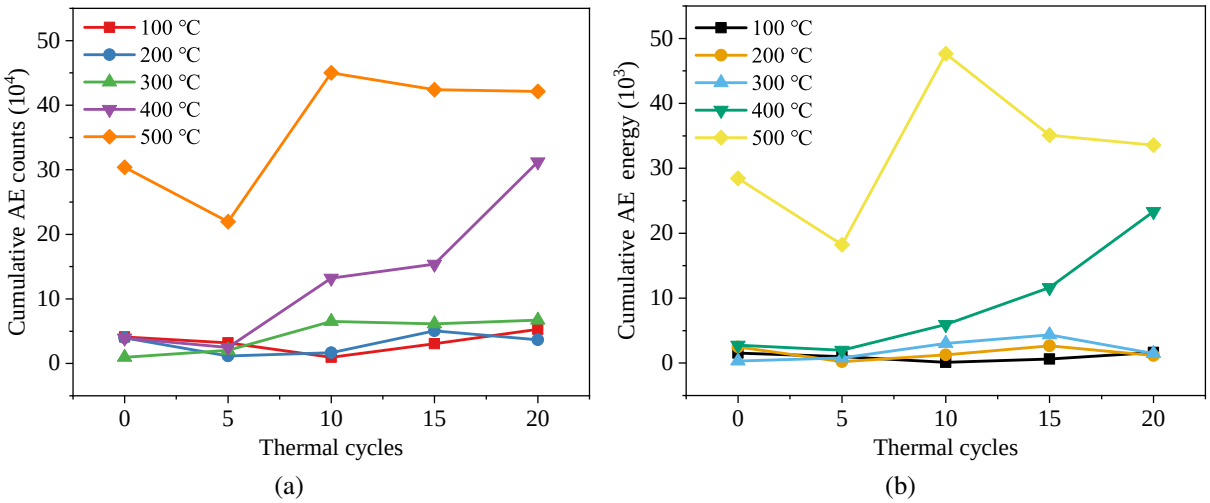

Fig. 8. Relationships between (a) cumulative AE count and (b) cumulative AE energy with respect to the number of thermal shocks (cycles).

internal damage accumulated to a certain degree, and all cracks were almost connected. The specimen was abruptly damaged (i.e., failure) when the granite's strength limit was surpassed by the stress.

As the number of seawater fatigue thermal shocks rises, both the cumulative AE count and its initial growth rate progressively increase (Fig. 5). This trend suggests that the severity of damage within the specimen grows with the number of thermal shocks, leading to more complete crack development and a reduction in the ultimate tensile strength of the specimen. In Fig. 6, with rising heat treatment temperature, the damage duration is extended. And the AE count rises gradually as specimen approaches the ultimate tensile stress, whereas the occurrence of a larger AE count gradually decreased. This observation suggests that the specimen's brittleness has decreased and its ductility has increased, leading to extended time to specimen failure. And the specimen is ultimately destroyed by the accumulation of micro-cracks under load to form a larger macroscopic crack.

3.4 Cumulative AE count and cumulative AE energy

AE energy serves as a crucial indicator of AE activity level and microcrack strength (Wang et al., 2016). Figs. 7 and 8 depict the variations in cumulative AE count and energy across varying heat treatment temperatures (Fig. 7) and various numbers of seawater thermal shocks (Fig. 8). The data were collected during the Brazilian splitting tests.

The cumulative counts and cumulative energy exhibited similar curves in response to changes in heating temperature and the quantity of thermal shocks. There was a general upward trend in cumulative counts and cumulative energy in varying quantities of thermal shocks with increasing temperature (Fig. 7). However, the temperatures at which these cumulative measures began to rise significantly varied depending

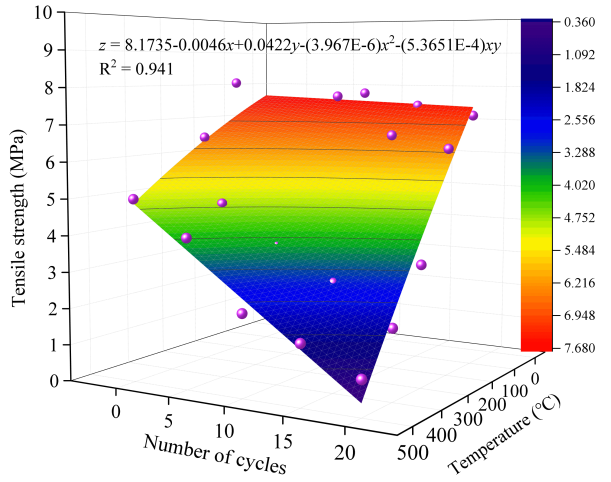

Fig. 9. The non-linear surface fitting between tensile strength and the number of thermal shocks (cycles) and treatment temperature.

on the number of thermal shock cycles. For 0-5 cycles, the temperature of significant increases that start to happen in cumulative counts and cumulative energy was observed at 400 °C, whereas for 10-20 cycles, this threshold dropped to 300 °C or lower. This indicates that in lower the number of cycles condition, it needs higher temperatures to start significant increases in cumulative counts and energy, and the specimen also need higher temperatures to occur severe damage.

The cumulative AE counts and energy showed no significant change when the treatment temperature was 300 °C or lower (Fig. 8). Within this range, the specimens exhibited low AE activity, incomplete micro crack development, slight variations in tensile strength, and less effect from treatment temperature and the quantity of thermal shocks. The cumulative AE count and energy were more affected by the number of thermal shocks when the treatment temperature was between 400 and 500 °C. A trend of significant increase was observed after 5-10 thermal shocks. Between 10 and 20 thermal shocks, the cumulative counts and energy continued to rise at a treatment temperature of 400 °C but started to decrease at a temperature treatment of 500 °C. Nonetheless, at varying numbers of seawater thermal and treatment temperatures, the cumulative counts and cumulative energy reached their peak, particularly at a temperature of 500 °C.

The aforementioned observations suggest that relative to the heating temperature, the quantity of thermal shocks exerts less influence, and high-temperature treatment significantly affects the damage to a specimen. The frequency of the thermal shocks from seawater progressively increases its impact on a specimen under high-temperature treatment, potentially generating more microcracks in the specimen during loading.

4. Discussion

4.1 Tensile strength spatial fitting

The non-linear surface fitting of different numbers of seawater thermal shocks and heat treatment temperature with the tensile strength in the current research are presented in Fig. 9. The fitting equation and correlation coefficient are also provided in Fig. 9. And the temperature and the number of cycles are denoted as the independent variables x and y respectively, while the tensile strength represents the dependent variable z.

As depicted by the spatial equation fitting correlation in Fig. 9, the nonlinear surface has a better fit. The nonlinearly fitted surface demonstrates a distinct shift from high to low as both the number of cycles and temperature increase. Additionally, the parameters are individually associated with the heat treatment temperature in the fitted curve exhibit negative values, while the parameter related to cycles alone is positive. This suggests a stronger negative correlation between tensile strength and heat treatment temperature compared to cycles. However, the negative value of the parameter linking temperature to cycles suggests that heat treatment temperature promotes the deterioration of granite by seawater thermal shocks. This relationship emphasizes how crucial it is to carry out additional research on how seawater thermal shock and heat treatment temperature affect granite.The spatial fitting equation presented in Fig. 9 enables the prediction of the effect of the number of seawater thermal shocks and heat treatment temperature on granite tensile strength.

4.2 Damage patterns

RA/AF values, among the AE waveform metrics, enable the qualitative examination of rupture mechanisms (Nejati et al., 2018; Zhou et al., 2022). Gan et al. (2020) proposed a tension-shear rupture determination value of 90 for AF/RA in the Brazilian splitting test of granite, according to the judgment results of RA and AF values, and the matrix tensor judgment results proposed by Ohtsu (1991), Ohno and Ohtsu (2010). Additionally, the crack classification of granite based on Kneedle's algorithm with AF/RA as the 112.5 demarcation slope was measured by Wang et al. (2024). Taken together, we use an AF/RA value of 100 as the threshold value for determining tension-shear rupture in granite.

The AF/RA values of the test specimens exposed to 5 thermal shocks and a treatment temperature of 500 °C are used as typical examples to assess the impact of cycles and treatment temperature on the damage pattern. Fig. 10 illustrates the AF-RA plots for both 5 and 20 thermal shocks at a specific 500 °C. Additionally, Table 1 summarizes the percentage of AF/RA greater than and less than 100 events for typical examples. For test specimens exposed to 5 thermal shocks and heat treatment temperatures of 100, 200, 300, 400 and 500 °C, the measured AF/RA events exceeding 100 comprised 85.4%, 90.0%, 88.9%, 72.8% and 69.7% of the total number of observations, respectively. These results suggest that the treatment temperature exerted minimal influence on the internal structure of the granite when the number of seawater thermal shocks was small, and granite damage was primarily influenced by tensile damage. In the AE analysis, the number of events with AF/RA exceeding 100, produced by the test specimens after 0, 5, 10, 15, and 20 thermal shock cycles at a treatment temperature of 500 °C, comprised 77.5%, 69.7%, 56.9%, 39.7%, and 19.5% of the events that took place

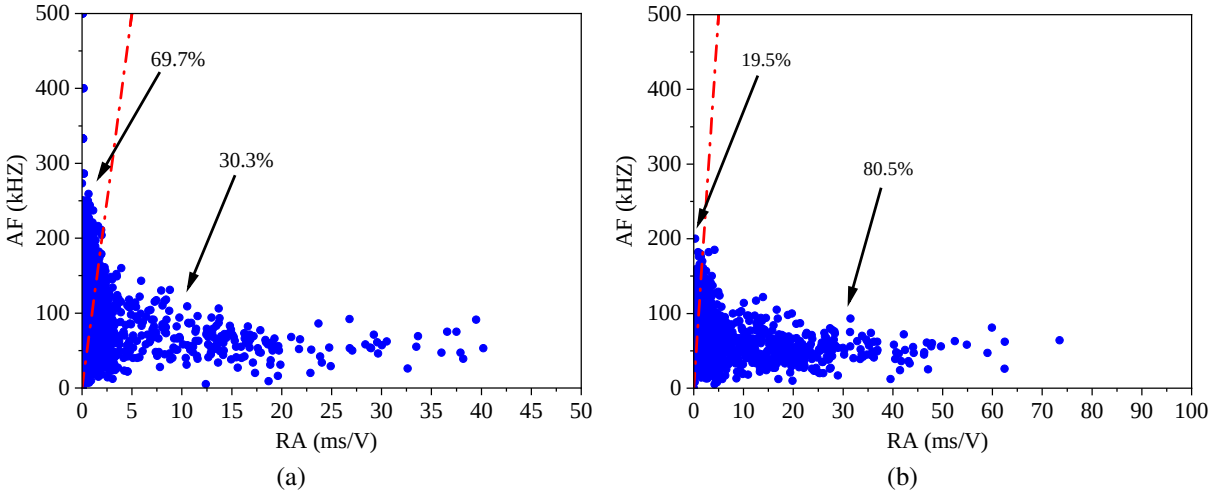

Fig. 10. An analysis of AE waveform parameters, specifically AF values against RA values for granite test specimens exposed to 500 °C treatment temperature and different numbers of thermal shock cycles. (a) 5 and (b) 20 cycles.

Table 1. Summary of percentage of events with AF/RA above and below 100 for typical examples.

No.	Heat treatment temperature (°C)	Numbers of thermal shock cycles	Percentage of AF/RA $\leq$ 100	Percentage of AF/RA $>$ 100
S1	100	5	85.4	14.6
S2	200	5	90.0	10.0
S3	300	5	88.9	11.1
S4	400	5	72.8	27.2
S5	500	5	69.7	30.3
C0	500	0	77.5	22.5
C10	500	10	56.9	43.1
C15	500	15	39.7	60.3
C20	500	20	19.5	80.5

overall, respectively. This finding indicates that tensile damage and shear damage coexist during the damage process within the specimens. Granite's interior structure is more severely impacted when it is subjected to high temperatures and cold seawater thermal shocks. As the cycles increase, the specimens gradually transitioned from tension damage to shear damage in the Brazilian splitting experiments.

4.3 Granite damage parameter (*D*)

Currently, the elastic modulus, energy density, and other variables can be used to express damage, on the basis of the stress-strain curve. Ran et al. (2023) used the strain energy of dissipated energy to define the damage variable. This study employs acoustic emission variables, examining the degree of damage in a rock by using the ringing number (Zhang et al., 2017). A damage parameter (D) can be defined based on AE cumulative counts:

$$D = \frac{\Omega}{\Omega_m} \tag{1}$$

where Ω_m represents the cumulative AE count corresponding to the final complete damage of a test granite specimen for a specific number of thermal shocks at a particular treatment temperature, and Ω is the cumulative AE count corresponding to the loading time of the granite under similar conditions.

The damage parameter D was calculated against time under varying numbers of thermal shocks and treatment temperatures of 100 and 500 °C to evaluate the impacts of seawater thermal shock count and treatment temperature on granite damage (Fig. 11). At a treatment temperature of 100 °C (Fig. 11(a)), the granite damage variable D changed with time along smooth curves, and the growth rate of D gradually increased until the final slope resembled a vertical line. This behavior suggests that the granite was less affected by temperature damage during this period, and the damage to the specimens accumulated slowly from the initial damage to the final rapid, brittle crack in Brazilian cleavage. By contrasting the damage curves of specimens subjected to different numbers of thermal shocks, all specimens treated at 100 °C, different numbers of seawater thermal shocks led to varying degrees of damage to the granite. The final damage times of specimens exposed to varying quantities of thermal shocks varied, highlighting the increased visibility of the impacts of thermal shocks and seawater dissolving on granite at high temperatures.

In contrast, the damage curves of specimens exposed to 500 °C exhibited linear steps (Fig. 11(b)) rather than smooth curves. This pattern suggests that the granite was more significantly influenced by temperature damage due to the high treatment temperature of 500 °C, and these specimens exhibited more ductile characteristics. During the initial loading phase, the specimens' damage variable D showed the highest growth rate, indicating severe internal damage to the specimens and the presence of a larger number of cracks before loading. Consequently, these specimens developed and produced internal

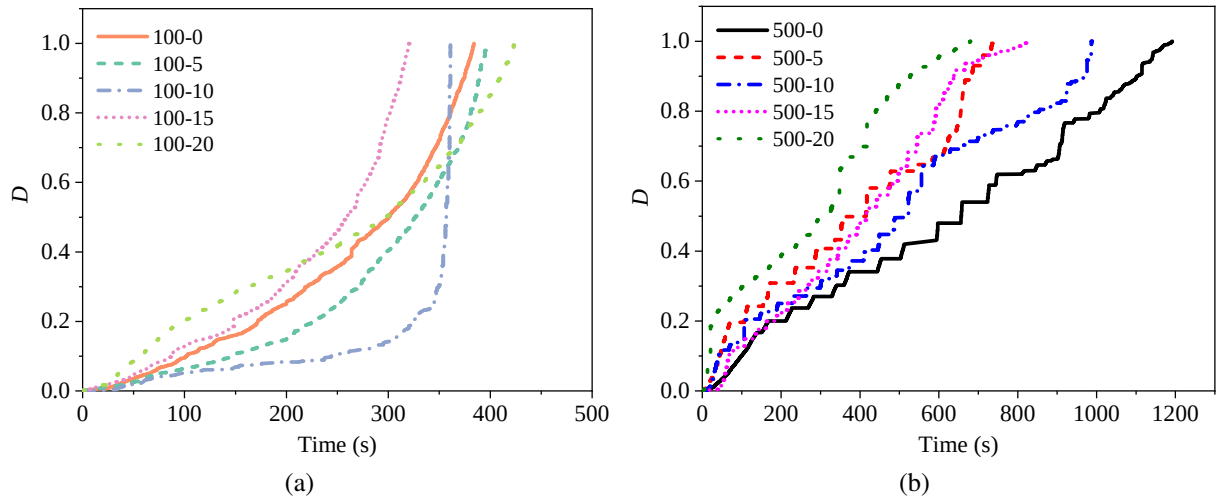

Fig. 11. Damage parameter *D*, plotted against time, for varying numbers of thermal shocks and treatment temperatures of (a) 100 °C and (b) 500 °C.

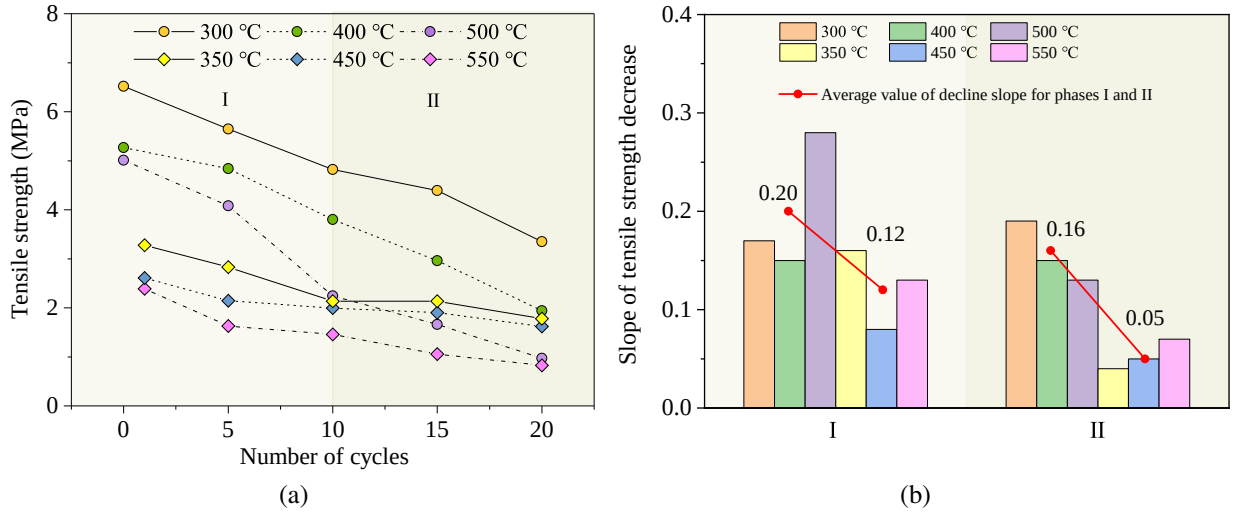

Fig. 12. (a) Tensile strength curves under different numbers of seawater and freshwater thermal shocks (cycles) and (b) Slope of tensile strength decrease under different numbers of seawater and freshwater thermal shocks (cycles) in stages I and II (Zhu et al., 2020a).

cracks violently when they were first loaded. With increasing loading time, the damage curve of the specimen showed a stepped shape, finally transitioning to a curve resembling a linear pattern. This change indicates that the specimen entered a stage of damage accumulation, and with the compression and expansion of its internal pores, underwent ductile damage.

A comparison of the damage curves for varying quantities of thermal shocks at the treatment temperature of 500 °C reveals that as the quantity of thermal shocks increased, the time corresponding to the specimen's ultimate damage decreased. This finding suggests that the damage to the specimens originated from three sources: Treatment temperature, seawater dissolution, and the quantity of thermal shocks. The three processes subjected the specimens to increasing damage, reducing the time to reach the ultimate loading capacity of the specimens.

In order to highlight how seawater heat shock affects granite's tensile characteristics and damage effects, we compared our results with those from freshwater thermal shock tests (Zhu et al., 2020a) (Fig. 12). The low-cycle state is defined as the first stage (0-10 cycles) and the high-cycle state as the second stage (10-20 cycles). The tensile strength decreases quickly in the first stage, as Fig. 12(a) illustrates, and then stabilizes in the second stage as the number of freshwater cycles increases. In contrast, the tensile strength continuously shows a rather stable declining pattern under seawater cycles. The quantitative results in Fig. 12(b) illustrate that the average tensile strength's decreasing slopes in the first stage for seawater and freshwater are 0.20 and 0.12, respectively, indicating that seawater weakens the tensile strength of granite approximately 1.67 times more than freshwater. In the second stage, the decreasing slopes for seawater and freshwater are 0.16 and 0.05, respec-

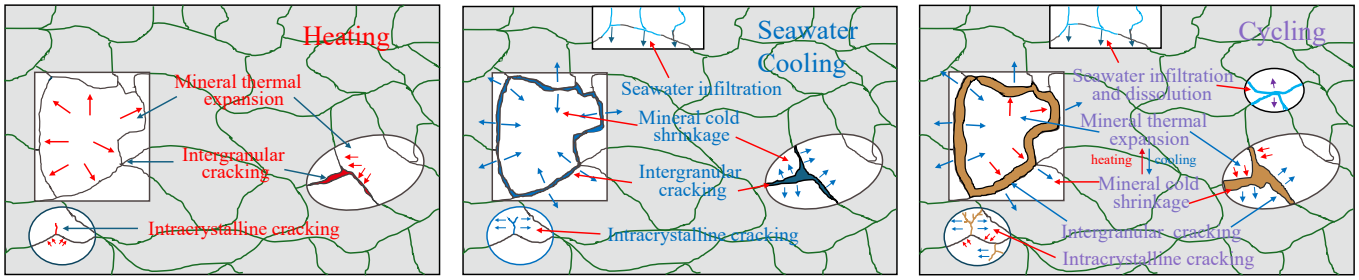

(a) (b) (c)

Fig. 13. Conceptual diagrams illustrating granite damage under the action of heating-seawater cooling cycles. (a) heating, (b) seawater cooling and (c) cycling.

Table 2. Potential chemical reactions between seawater and high-temperature granite (Yang et al., 2022).

Mineral phase	Processes of chemical reactions
K-feldspar	$KAlSi_3O_8 + 8H_2O \rightleftharpoons 3H_4SiO_4 + Al(HO)_4^- + K^+$
Albite	$NaAlSi_3O_8 + 8H_2O \rightleftharpoons 3H_4SiO_4 + Al(OH)_4^- + Na^+$
Quartz	$SiO_2 + 2H_2O \rightleftharpoons H_4SiO_4$
Biotite	$KMg_3AlSi_3O_{10}(OH)_2 + 6H^+ \rightleftharpoons 3H_4SiO_4 + Al(OH)_4 + 3Mg^{2+} + K^+$
Muscovite	$KAl_3Si_3O_{10}(OH)_2 + 10H^+ = 3H_4SiO_4 + 3Al^{3+} + K^+$
Calcite	$CaCO_3 \rightleftharpoons CO_3^{2-} + Ca^{2+}$
Gypsum	$CaSO_4 \cdot {}_2H_2O \rightleftharpoons 2H_2O + SO_4^{2-} + Ca^{2+}$
Chlorite	$Mg_5Al_2Si_3O_{10}(OH)_8 + 16H^+ = 3H_4SiO_4 + 6H_2O + 2Al^{3+} + 5Mg^{2+}$

tively, with seawater weakening the tensile strength about 3.20 times more than freshwater. This analysis demonstrates that seawater thermal shock causes more pronounced deterioration of granite compared to freshwater, particularly during high cycles (10-20) and at high temperatures (300 to 500 °C).

Based on the experimental findings and the analysis of previous research, we delve into the degradation mechanism of seawater thermal shock on granite. Table 2 lists several potential chemical reactions between seawater and high-temperature granite to elucidate the composition of granite and seawater. These reactions between seawater and granite are characterized by the precipitation of positive ions and mineral dissolution processes, compared with freshwater cooling. In terms of the damage inflicted on granite by seawater thermal shock, Fig. 13 presents a conceptual summary of the damage to a specimen, based on exposure temperature and seawater cold cycling. Sirdesai et al. (2017) emphasized significant variations in the rates of thermal expansion of various minerals within a section of rock, which is the primary cause of the deterioration of its mechanical characteristics. As illustrated in Fig. 13(a), the specimen's mineral particles showed noticeably uneven expansion as the treatment temperature increased (Sun et al., 2015), and the specimens were heated to produce internal stresses from the rock's uneven expansion, which caused intergranular cracks to form and, eventually, crystal cracks. Hu et al. (2024) demonstrated that low-temperature seawater cooling the high-temperature granite can induce a significant thermal shock fatigue effect, resulting in a notable increase in the rock's overall porosity and permeability. The application of cold seawater generates a thermal shock within the specimen, accompanied by mineral shrinkage. At this stage, intergranular cracks and crystal cracks expand and extend, while seawater begins to penetrate the specimen (Fig. 13(b)). Eventually, as in Fig. 13(c), with a new cycle, additional cracks form, old intergranular and crystal cracks further develop, and seawater penetrates these cracks, initiating mineral dissolution. This process contributes to increased porosity and damage within the specimen. The effectiveness of heat extraction from hot dry rock in EGS is significantly improved by this process.

However, it is noteworthy that the precipitation of negative ions during the thermal shock of seawater and granite may exert a beneficial effect on granite, as demonstrated by the secondary minerals that are produced during their chemical interactions, including calcite, gypsum, and chlorite. This process explains why granite's tensile strength increases as the quantity of seawater cycles increases at temperatures between 100 and 200 °C. The underlying mechanism is that at these relatively low temperatures, the thermal shock induced by seawater incurs minimal damage to the granite. Simultaneously, the formation of secondary minerals effectively fills the pores within the granite, thereby augmenting the tensile strength of the specimens. These research findings contribute to advancing the use of seawater as a heat extraction medium for hot dry rocks. However, there are still many aspects awaiting further exploration regarding the utilization of seawater as a medium of heat extraction for HDR. The discussions aim

to provide valuable insights into the temperature-dependent behavior of granite specimens and underscore the critical role of the variable D in characterizing incurred damage.

5. Conclusions

The current research is focused on examining the stretching behavior and granite damage mechanisms in response to various treatment temperatures (100, 200, 300, 400 and 500 °C) and various numbers of seawater thermal shocks (0, 5, 10, 15 and 20). An analysis of AE signal parameters is conducted to provide insights into the damage progression and modes in test granite under different loading conditions. The research yielded the following conclusions:

1) The tensile strength of granite is mainly influenced by treatment temperature, the number of thermal shocks, and seawater dissolution. When the temperature exceeds the heat treatment threshold of 200 °C, the coupled effects of thermal shock and seawater chemistry significantly accelerate the deterioration of granite, much more than freshwater.
2) The internal damage of granite is highly correlated with its tensile strength, and both cumulative counts and cumulative energy exhibit similar trends with changes. As the treatment temperature and the number of seawater thermal shocks increase, the cumulative count and cumulative energy of granite rise, resulting in more fully developed cracks within the granite specimens and lower tensile strength.
3) There exists a robust negative relationship between the granite's tensile strength, the number of seawater thermal shock cycles, and the heat treatment temperature. Notably, individually subjecting granite to thermal shock cycles with seawater may enhance its strength, however, the temperature effectively promotes the deterioration of granite by seawater thermal shock, thereby amplifying the adverse relationship between the frequency of seawater thermal shocks and tensile strength.
4) The damage pattern of granite is significantly influenced by both heat treatment temperature and seawater cold cycling, with their interaction being more pronounced than that of temperature alone. As the temperature rises, tensile failure is still the predominant mode of granite damage. However, as the seawater fatigue thermal shock intensifies, there is a gradual transition in granite damage from predominantly tensile to predominantly shear failure.
5) The damage parameter D effectively corresponds to the degree of damage induced by varying temperatures and different numbers of thermal shocks from seawater during loading. As temperature rises, the damage curve changes from smooth to stepped, which is equivalent to the rocks changing from brittle to plastic. Meanwhile, granite becomes more porous as the quantity of thermal shocks from seawater rises and the time from loading to the failure of the specimen decreases.

Acknowledgements

This study was funded by the National Natural Science Fund of China (Nos. U22A20166, 52304097 and 52192625), Young Elite Scientists Sponsorship Program by CAST (No. 2023QNRC001), Open Foundation of Key Laboratory of Deep Earth Science and Engineering (Sichuan University), and Ministry of Education (No. DUSE202301). The authors would also like to express their gratitude to their anonymous colleagues for their kind efforts and valuable comments for improving this work.

Conflict of interest

The authors declare no competing interest.

References

Asai, P., Panja, P., McLennan, J., et al. Efficient workflow for simulation of multifractured enhanced geothermal systems (EGS). Renewable Energy, 2019, 131: 763-777.

Bertani, R. Geothermal power generation in the world 2010-2014 update report. Geothermics, 2016, 60: 31-43.

Breede, K., Dzebisashvili, K., Liu, X., et al. A systematic review of enhanced (or engineered) geothermal systems: Past, present and future. Geothermal Energy, 2013, 1: 4.

Chen, C., Chu, P., Xie, H., et al. Fracture behavior of high-temperature granite subjected to liquid nitrogen cooling: Semi-circular bending test and crack evolution analysis. Theoretical and Applied Fracture Mechanics, 2023, 128: 104100.

Chen, Y., Wang, S., Ni, J., et al. An experimental study of the mechanical properties of granite after high temperature exposure based on mineral characteristics. Engineering Geology, 2017, 220: 234-242.

Deng, H., Hu, J., Liu, G., et al. Study on the surface morphology and fractal characteristics of granite under thermal shock of seawater. Thermal Science, 2023, 27: 571-579.

Ding, Q., Ju, F., Mao, X., et al. Experimental investigation of the mechanical behavior in unloading conditions of sandstone after high-temperature treatment. Rock Mechanics and Rock Engineering, 2016, 49: 2641-2653.

Filipussi, D. A., Guzman, C. A., Xargay, H. D., et al. Study of acoustic emission in a compression test of andesite rock. Procedia Materials Science, 2015, 9: 292-297.

Gan, Y., Wu, S., Ren, Y., et al. Research on the evaluation index of granite splitting damage based on acoustic emission rise time/ampitude and average frequency value. Rock and Soil Mechanics, 2020, 41(7): 2324-2332. (in Chinese)

Gautam, P. K., Verma, A. K., Jha, M. K., et al. Effect of high temperature on physical and mechanical properties of Jalore granite. Journal of Applied Geophysics, 2018, 159: 460-474.

Gérard, A., Genter, A., Kohl, T., et al. The deep EGS (Enhanced Geothermal System) project at Soultz-sous-

Forêts, Alsace, France. Geothermics, 2006, 35(5-6): 473-714.

Ge, Z., Sun, Q. Acoustic emission (AE) characteristics of granite after heating and cooling cycles. Engineering Fracture Mechanics, 2018, 200: 418-429.

Huang, S. P. COMMENTARY: Geothermal energy in China. Nature Climate Change, 2012, 2(8): 557-560.

Hu, J., Xie, H., Gao, M., et al. Damage mechanism and heat transfer characteristics of limestone after thermal shock cycle treatments based on geothermal development. International Journal of Rock Mechanics and Mining Sciences, 2022, 160: 105269.

Hu, J., Xie, H., Li, C., et al. Effect of cyclic thermal shock on granite pore permeability. Lithosphere, 2021, 2021(Special 5): 4296301.

Hu, J., Xie, H., Li, C., et al. Evolution mechanism of permeability of hot dry rock under coupled effect of thermal fatigue and seawater interaction during coastal geothermal development. Renewable and Sustainable Energy Reviews, 2024, 189: 114061.

Kumari, W. G. P., Ranjith, P. G., Perera, M. S. A., et al. Temperature-dependent mechanical behaviour of Australian Strathbogie granite with different cooling treatments. Engineering Geology, 2017, 229: 31-44.

Kumari, W. G. P., Ranjith, P. G., Perera, M. S. A., et al. Hydraulic fracturing under high temperature and pressure conditions with micro CT applications: Geothermal energy from hot dry rocks. Fuel, 2018a, 230: 138-154.

Kumari, W. G. P., Ranjith, P. G., Perera, M. S. A., et al. Experimental investigation of quenching effect on mechanical, microstructural and flow characteristics of reservoir rocks: Thermal stimulation method for geothermal energy extraction. Journal of Petroleum Science and Engineering, 2018b, 162: 419-433.

Li, H., Jiang, X., Xu, Z., et al. The effect of supercritical CO_2 on failure mechanisms of hot dry rock. Advances in Geo-Energy Research, 2022, 6(4): 324-333.

Li, N., Zhang, S., Ma, X., et al. Thermal effect on the evolution of hydraulic fracture conductivity: An experimental study of enhanced geothermal system. Journal of Petroleum Science and Engineering, 2020, 187: 106814.

Ma, W., Yang, C., Ahmed, S. F., et al. Effects of thermophysical parameters of fracturing fluid on hot dry rock damage in hydraulic fracturing. Geomechanics for Energy and the Environment, 2022, 32: 100405.

Nejati, H. R., Nazerigivi, A., Sayadi, A. R. Physical and mechanical phenomena associated with rock failure in Brazilian Disc Specimens. International Journal of Geological and Environmental Engineering, 2018, 12(1): 35-39.

Ohno, K., Ohtsu, M. Crack classification in concrete based on acoustic emission. Construction and Building Materials, 2010, 24(12): 2339-2346.

Ohtsu, M. Simplified moment tensor analysis and unified decomposition of acoustic emission source: application to in situ hydrofracturing test. Journal of Geophysical Research: Solid Earth, 1991, 96(B4): 6211-6221.

Pan, S., Gao, M., Shah, K., et al. Establishment of enhanced geothermal energy utilization plans: Barriers and strategies. Renewable Energy, 2019, 132: 19-32.

Pathiranagei, S. V., Gratchev, I., Kong, R. Engineering properties of four different rocks after heat treatment. Geomechanics and Geophysics for Geo-Energy and Geo-Resources, 2021, 7(1): 16.

Ran, Q., Chen, P., Liang, Y., et al. Hardening-damage evolutionary mechanism of sandstone under multi-level cyclic loading. Engineering Fracture Mechanics, 2024, 307: 110291.

Ran, Q., Liang, Y., Zou, Q., et al. Experimental investigation on mechanical characteristics of red sandstone under graded cyclic loading and its inspirations for stability of overlying strata. Geomechanics and Geophysics for Geo-Energy and Geo-Resources, 2023, 9(1): 11.

Rong, G., Peng, J., Cai, M., et al. Experimental investigation of thermal cycling effect on physical and mechanical properties of bedrocks in geothermal fields. Applied Thermal Engineering, 2018, 141: 174-185.

Sagar, R. V., Prasad, B. K. R., Kumar, S. S. An experimental study on cracking evolution in concrete and cement mortar by the b-value analysis of acoustic emission technique. Cement and Concrete Research, 2012, 42(8): 1094-1104.

Salimzadeh, S., Nick, H. M., Zimmerman, R. W. Thermoporoelastic effects during heat extraction from low-permeability reservoirs. Energy, 2018, 142: 546-558.

Shao, Z., Sun, L., Aboayanah, K. R., et al. Investigate the mode I fracture characteristics of granite after heating/-LN_2 cooling treatments. Rock Mechanics and Rock Engineering, 2022, 55: 4477-4496.

Sha, S., Rong, G., Chen, Z. H., et al. Experimental evaluation of physical and mechanical properties of geothermal reservoir rock after different cooling treatments. Rock Mechanics and Rock Engineering, 2020, 53(11): 4967-4991.

Shi, X., Jing, H., Yin, Q., et al. Investigation on physical and mechanical properties of bedded sandstone after high-temperature exposure. Bulletin of Engineering Geology and the Environment, 2020, 79: 2591-2606.

Siratovich, P. A., Villeneuve, M. C., Cole, J. W., et al. Saturated heating and quenching of three crustal rocks and implications for thermal stimulation of permeability in geothermal reservoirs. International Journal of Rock Mechanics and Mining Sciences, 2015, 80: 265-280.

Sirdesai, N. N., Singh, T. N., Ranjith, P. G., et al. Effect of varied durations of thermal treatment on the tensile strength of red sandstone. Rock Mechanics and Rock Engineering, 2017, 50: 205-213.

Sun, Q., Zhang, W., Xue, L., et al. Thermal damage pattern and thresholds of granite. Environmental Earth Sciences, 2015, 74: 2341-2349.

Van Berk, W., Fu, Y., Schulz, H. M. Temporal and spatial development of scaling in reservoir aquifers triggered by seawater injection: Three-dimensional reactive mass transport modeling of water-rock-gas interactions. Journal of Petroleum Science and Engineering, 2015, 135: 206-217.

Venturini, A. M. R., Dulieu-Barton, J. M. Initial studies for AE characterisation of damage in composite materials. Advanced Materials Research, 2006, 13-14: 273-280.

Wang, J., Liang, P., Zhang, Y., et al. Classification of rock tension-shear fracture based on acoustic emission RA-AF values with kneedle algorithm. Chinese Journal of Rock Mechanics and Engineering, 2024, 43(S1): 3267-3279. (in Chinese)

Wang, J., Xie, L., Xie, H., et al. Effect of layer orientation on acoustic emission characteristics of anisotropic shale in Brazilian tests. Journal of Natural Gas Science and Engineering, 2016, 36: 1120-1129.

Watanabe, H., Murakami, Y., Ohtsu, M. Quantitative evaluation of damage in concrete based on AE. Zairyo, 2001, 50(12): 1370-1374. (in Japanese)

Weng, L., Wu, Z., Liu, Q. Influence of heating/cooling cycles on the micro/macrocracking characteristics of Rucheng granite under unconfined compression. Bulletin of Engineering Geology and the Environment, 2020, 79: 1289-1309.

Xi, Y., Wang, H., Jiang, J., et al. Impacts of different cooling methods on the dynamic tensile properties of thermal-treated granite. International Journal of Rock Mechanics and Mining Sciences, 2023, 169: 105438.

Yang, F., Wang, G., Hu, D., et al. Influence of water-rock interaction on permeability and heat conductivity of granite under high temperature and pressure conditions. Geothermics, 2022, 100: 102347.

Yang, S., Ranjith, P. G., Jing, H., et al. An experimental investigation on thermal damage and failure mechanical behavior of granite after exposure to different high temperature treatments. Geothermics, 2017, 65: 180-197.

Yin, Q., Jing, H., Liu, R., et al. Pore characteristics and nonlinear flow behaviors of granite exposed to high temperature. Bulletin of Engineering Geology and the Environment, 2020, 79: 1239-1257.

Yin, Q., Wu, J., Jiang, Z., et al. Investigating the effect of water quenching cycles on mechanical behaviors for granites after conventional triaxial compression. Geomechanics and Geophysics for Geo-Energy and Geo-Resources, 2022, 8(2): 77.

Yin, Q., Wu, J., Zhu, C., et al. The role of multiple heating and water cooling cycles on physical and mechanical responses of granite rocks. Geomechanics and Geophysics for Geo-Energy and Geo-Resources, 2021, 7(3): 69.

Yu, P., Pan, P. Z., Feng, G., et al. Physico-mechanical properties of granite after cyclic thermal shock. Journal of Rock Mechanics and Geotechnical Engineering, 2020, 12(4): 693-706.

Zhang, B., Tian, H., Dou, B., et al. Macroscopic and microscopic experimental research on granite properties after high-temperature and water-cooling cycles. Geothermics, 2021, 93: 102079.

Zhang, R., Ai, T., Gao, M., et al. Basic Theory and Experimental Research on Rock Acoustic Emission. Chengdu, China, Sichuan University Press, 2017. (in Chinese)

Zhang, W., Guo, T., Qu, Z., et al. Research of fracture initiation and propagation in HDR fracturing under thermal stress from meso-damage perspective. Energy, 2019, 178: 508-521.

Zhao, F., Sun, Q., Zhang, W. Thermal damage analysis based on physical and mechanical indices of granodiorite. Géotechnique Letters, 2020, 10(2): 250-255.

Zhou, C., Gao, F., Cai, C., et al. Effect of different cooling treatments on the tensile properties and fracture modes of granite heated at different temperatures. Natural Resources Research, 2022, 31(2): 817-833.

Zhu, D., Fan, Y., Liu, X., et al. Characteristics of acoustic emission response during granite splitting after high temperature-water cooling cycles. Sustainability, 2022, 14(20): 13601.

Zhu, D., Jing, H., Yin, Q., et al. Experimental study on the damage of granite by acoustic emission after cyclic heating and cooling with circulating water. Processes, 2018, 6(8): 101.

Zhu, D., Jing, H., Yin, Q., et al. Mechanical characteristics of granite after heating and water-cooling cycles. Rock Mechanics and Rock Engineering, 2020a, 53: 2015-2025.

Zhu, Z., Ranjith, P. G., Tian, H., et al. Relationships between P-wave velocity and mechanical properties of granite after exposure to different cyclic heating and water cooling treatments. Renewable Energy, 2021, 168: 375-392.

Zhu, Z., Tian, H., Chen, J., et al. Experimental investigation of thermal cycling effect on physical and mechanical properties of heated granite after water cooling. Bulletin of Engineering Geology and the Environment, 2020b, 79: 2457-2465.

Zolfaghari, S. M., Soltani, M., Hosseinpour, M., et al. Comprehensive analysis of geothermal energy integration with heavy oil upgrading in hot compressed water. Applied Energy, 2023, 345: 121260.

Zuo, J., Zhou, H., Fang, Y., et al. Experimental study on thermal cracking of deep granite in the Beishan region of Gansu. Chinese Journal of Rock Mechanics and Engineering, 2011, 30(6): 1107-1115. (in Chinese)